UNIVERSITY OF MARYLAND

Observing marine heatwaves in the Chesapeake Bay using satellite sea surface temperature

Rachel Wegener

Under the advisorship of Dr. Veronica Lance and Dr. Jacob Wenegrat

A scholarly paper in partial fulfillment of the requirements for the degree of

Master of Science

DEPARTMENT OF ATMOSPHERIC AND OCEANIC SCIENCE

Contents

1. Introduction

Anthropogenic climate change is raising global temperatures, both through an increasing global average temperature and through an increasing number of extreme temperature events (Rahmstorf and Coumou 2011). One of these increasingly common extreme events is Marine Heatwaves (MHW), a prolonged period of anomalously warm water (Oliver, Burrows, et al. 2019). Extreme temperature changes such as MHW affect marine ecosystems on the individual, population, community level. Not all MHW are the same, however, and the ecosystem response depends on the characteristics of the MHW, such as the duration and rate of onset (Smith, Burrows, Hobday, King, et al. 2023). These ecosystem impacts translate into socioeconomic impacts. In the US alone economic losses through October 2022

"of single MHW events exceed US$800 million in direct losses and in excess of US$3.1 billion per annum in indirect losses for multiple consecutive years" (Smith, Burrows, Hobday, Sen Gupta, et al. 2021). MHWs and their ecological and economic impact are unfortunately part of our warming world.

These economic impacts are especially important in the ecologically productive coastal ocean and global estuaries. The Chesapeake Bay is the largest and one of the most productive estuaries in the United States (Bilkovic et al. 2019). The Chesapeake Bay has seen a trend of long term warming (Hinson et al. 2022) and increasing temperatures have been linked to growing hypoxic conditions in the Bay (Du et al. 2018). In addition to long term warming, previous work has identified MHWs in the Chesapeake Bay using buoy data (Mazzini and Pianca 2022). MHWs in 2006 caused an over 50% loss in the seagrass species *Z. marina* in which fisheries species find nursery habitat (Lefcheck et al. 2017). As a result, the area saw declines in three commercially important fish species (Smith, Burrows, Hobday, King, et al. 2023).

Here we show that satellite data can be used to study MHWs in the Chesapeake Bay. Satellite data provides spatial resolution that is not possible with buoy data alone. Past work in the Chesapeake Bay has shown spatial variation in the long term warming trend (Hinson et al. 2022), which suggests that there could be some spatial variation in the occurrence of extreme temperature events. We look not just at the spatial variation in the occurrence of MHW, but also show patterns in the characteristics of MHW, critical for assessing the potential ecological impact. Increased spatial resolution and clarity into regional trends in MHW characteristics benefits our understanding of extreme temperature events in the Chesapeake Bay and could benefit monitoring efforts that help mitigate the high economic impact and conserve protected waters.

2. Methods

2.1. Satellite Data Sources

The satellite data products suitable for this study are those with high spatial resolution and long time series. The need for high resolution is driven by the size of the Chesapeake Bay. The need for a long time series is driven by the baseline climatology required for MHW calculations. Hobday et al. 2016 recommends a 30 year climatology, but past work has shown that climatologies based on records as short as 10 years do not result in estimated MHW characteristics that differ appreciably from those calculated using the recommended 30 year time series (Schlegel, Oliver, Hobday, et al. 2019).

Two satellite SST products were evaluated: NASA MUR and NOAA Geopolar. NASA MUR is a daily ~1km level 4 product based on nighttime SST observations and provides an estimate of the foundation temperature (Chin, Vazquez-Cuervo, and Armstrong 2017). Foundation temperature, as defined by the Group for High Resolution Sea Surface Temperature (GHRSST), is the temperature at a depth free of diurnal variability (Beggs 2020). NOAA Geopolar is also a daily level 4 ~5km product (Maturi et al. 2017). Geopolar nighttime SST is used in order to avoid diurnal variation in the surface temperatures, thereby maintaining a SST definition that is comparable between Geopolar and MUR. See Table 1 for a summary of the two datasets. Both datasets are gap filled for clouds. There were still 7 days of missing data in the Geopolar dataset, which were removed by NOAA data processing due to quality control. These 7 days were linearly interpolated in each pixel when generating the climatologies.

Table 1. *Satellite Sea Surface Temperature (SST) Sources.*

Product Name	Version	Organization	Spatial Resolution	Temporal Resolution	Availability
MUR	4.1	NASA	0.01^o(~1 km)	daily	May 31, 2002 - present
Geopolar Blended	2.0	NOAA	0.05^o(~5 km)	daily	Sept 1, 2002 - present

2.2. Satellite Data Validation

In situ data compiled by the Chesapeake Bay Program (CBP)'s Water Quality Database was used to validate SST in the Chesapeake Bay. The database contains measurements from the CBP partner organizations at long-term, fixed-station monitoring programs. Traditional Partner Data from all the programs was used.

The satellite datasets both estimate foundation SST temperature. The in situ data, on the other hand, provides measurements of SST at several depths. To extract the foundation temperature values from the in situ dataset only the values explicitly labelled as not being in the very top or very bottom layers of the water column were retained. A single data point was selected from each sampling station that was closest to 2m depth, but not shallower than 0.2m or deeper than 8m. Data was used from January 1 2003 - December 31, 2019, the period over which we have SST for both the Geopolar and MUR datasets.

This processing produced about 34,000 in situ data points for comparison with the satellite data. Figure 1 shows the distribution of observations over time. There is a consistent seasonal sampling bias, in which summers are more highly sampled than winters. The black lines in Figure 1 show the average for each of the 17 calendar years. While there is some interannual variation, with a mean of 2,015 samples per year and standard deviation of 312 samples (11%), there is not a long term trend in the number of observations.

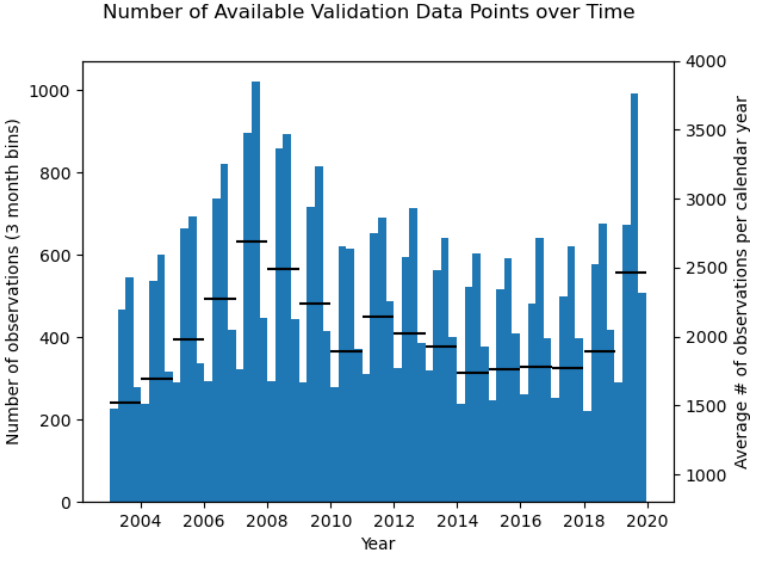

Figure 1. *Histogram of the number of observations, labelled on the left axis. There are 68 bins over the 17 year time series, producing 4 bins per year. The right axis shows the average number of observations in every calendar year. Each of the horizontal lines is present over Jan. - Dec. of the corresponding year.*

2.3. Marine Heatwave Calculation and Characteristics

Hobday et al. 2016 defines the canonical definition of a MHW: a MHW is an observed temperature that persists above the 90th percentile for at least 5 days. This is illustrated in Figure 2 panel A. The time period for the climatology is the full dataset time period, Jan. 1, 2003 - Dec. 31, 2023 (20 years). Again following Hobday et al. 2016, the 90th percentile threshold for each day uses the days from a centered 11 day window. After the threshold is calculated, the values are smoothed using a 31 day moving average. If multiple >5 day MHW occur within two days of each other they are considered to be a single MHW

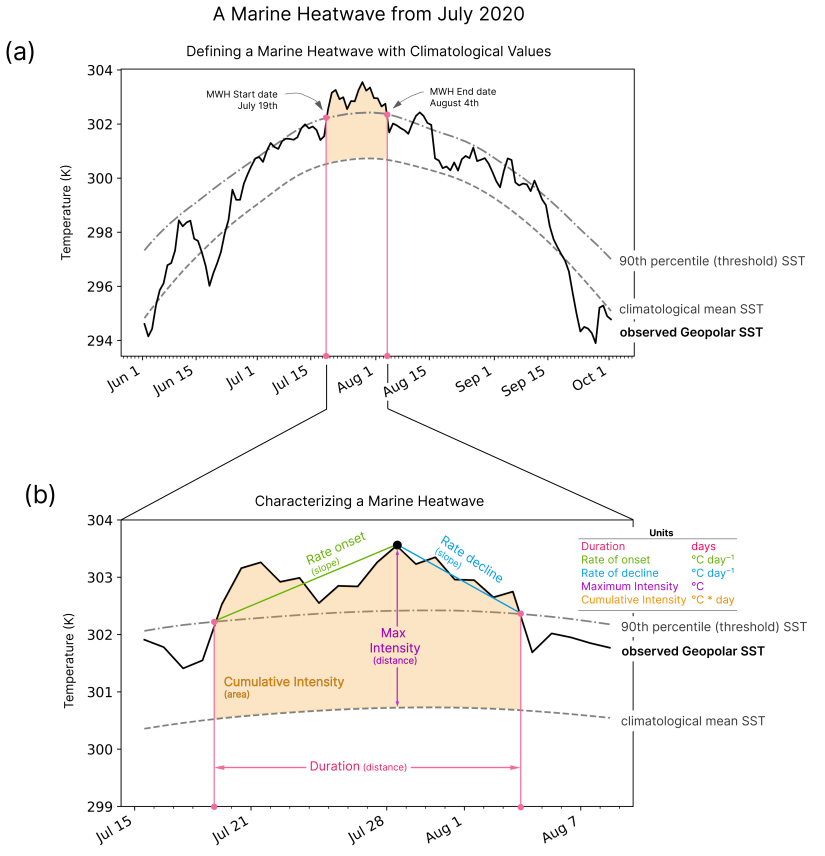

Figure 2. *The observed and climatological values of a MHW from July 2020 at* $38^o N$, $76^o W$. *Panel (a) visualizes a sustained period above the 90th percentile threshold value defining a MHW. Panel (b) shows SST focused on the heatwave period, labelling the 5 MHW statistics used in this study to characterize MHWs.*

event. MHW were calculated using the Python package marineHeatWaves. The details described above are the defaults of this package, and are consistent with the recommendations in Hobday et al. 2016. Geopolar and not NASA MUR was used to calculated MHW for reasons described in Section 3.1.4.

MHW characteristics allow us to better consider different types of MHW. The 5 characteristics analysed in this study are duration, rate of onset, rate of decline, maximum intensity, and cumulative intensity. Figure 2 panel B shows a graphic representation of these MHW characteristics for an example heatwave in July 2020. The definitions follow Hobday et al. 2016 and are also calculated using the marineHeatWaves package.

2.4. Aggregating Marine Heatwave Characteristics

MHW characteristics where aggregated across time into a single value for each pixel or spatial location (Figure 3). The six MHW characteristics were averaged over the 20 year time series to produce a single number per MHW characteristic. The process was repeated on each of the pixels in the Chesapeake Bay. The end result is a map of each of the 6 aggregated MHW characteristics across the Bay. In addition to the 6 aggregated characteristics in the diagram average intensity was considered, but was excluded because it was not found to be greatly different from the maximum intensity.

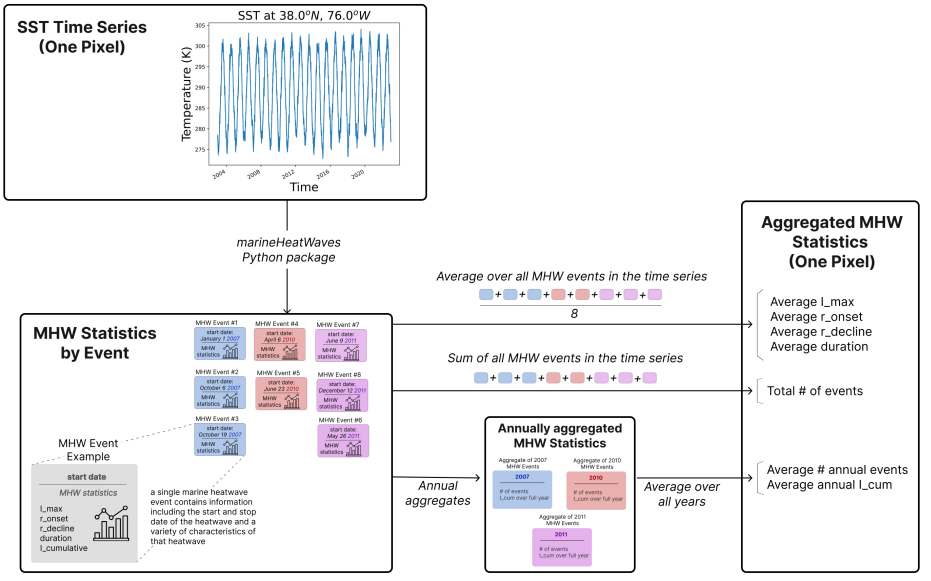

Figure 3. *The processing workflow completed for generating aggregated MHW characteristics. In the first step the Python package marineHeatWaves is used to calculate MHW events from a full SST time series at a single location. These events are then aggregated into a single value for that pixel using one of three routes shown on the figure.*

3. Results

3.1. Validation of Satellite SST in the Chesapeake Bay

Table 2. *Satellite Sea Surface Temperature (SST) Errors.*

Product Name	R^2	Slope	RMSE (^{o}C)
MUR	0.949	0.968	1.90
Geopolar Blended	0.958	0.949	1.72

Correlation coefficient, slope and root mean squared error (RMSE) quantify the mean error between the satellite and in situ SST estimates (summarized in Table 2). Results from the two satellite datasets were quantitatively similar, with Geopolar performing slightly better. Geopolar is slightly more consistent (larger R^2) and has a lower mean error (RMSE). These satellite errors do not account for observational errors or for errors in the process of choosing a foundation temperature depth from the CBP data.

While the mean satellite error provides a succinct summary, consideration of multiple forms of bias builds a more in depth understanding of the robustness of the results. In addition to the mean error metrics shown above, the following forms of potential error may also affect our results:

1. distribution of satellite error
2. spatial variability in satellite error
3. long term and seasonal variability in satellite error

We conclude with a brief discussion of the effects of the observed satellite errors on our MHW analysis.

3.1.1. Satellite Error Distributions

A histogram of errors in the satellite data shows that overall both satellites were too cold more often than they were too hot (Figure 4). In both datasets only a few highly erroneous data points lay outside of -10^oC - 7^oC, but MUR has more of these, perhaps contributing to the slightly higher RMSE.

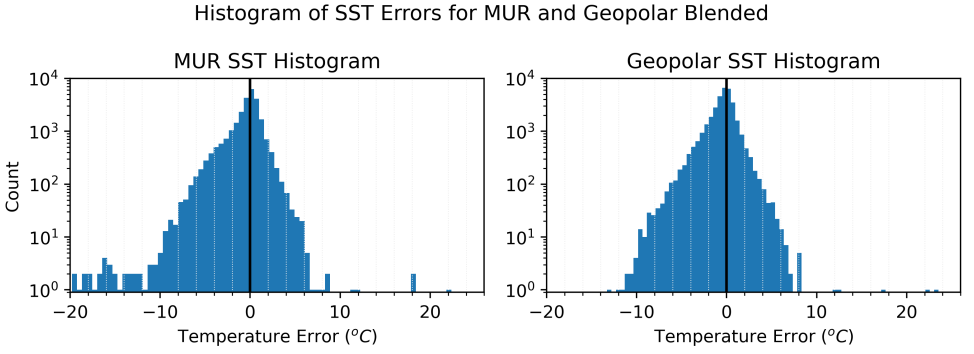

Figure 4. *Histograms of the temperature error for MUR SST and Geopolar SST, as compared to the Chesapeake Bay Program (CBP) in situ dataset. The left panel shows MUR and the right panel shows Geopolar. The x-axis shows in situ minus satellite SST, such that negative values represent satellite SST underestimates of in situ temperature. The y-axis shows the number of pixels with that level of error.*

3.1.2. Spatial Variability of Satellite Error

As the core of this investigation is discussion of the spatial distribution of MHW, spatial variability in the satellite errors was next considered. Figure 5 shows the 513 geographically unique sampling stations from the CBP data. At each location satellite errors for all observations at that location over time were averaged together. Both datasets are most accurate in the center of the Bay. Satellite error is the highest closest to the shoreline, most notably along the Potomac, Susquehanna and Gunpowder Rivers, where both satellites underestimate the temperature in those shoreline regions. MUR generally seems to perform better that Geopolar in the river inflow regions, perhaps a reflection of the higher spatial resolution of the MUR dataset.

One possible reason for higher satellite errors near shore is an adjacency effect. Recall that the satellite data are estimating nighttime temperature. At night, the land surface would tend to cool off faster than the surrounding water. Satellite pixels overlapping with land would then receive colder signal than pixels of pure water, thus making the pixel appear colder. Adjacency effects have been observed in ocean color satellites in a wide range of coastal environments (Bulgarelli and Zibordi 2018), as well as in the thermal infrared region over land (Duan et al. 2020).

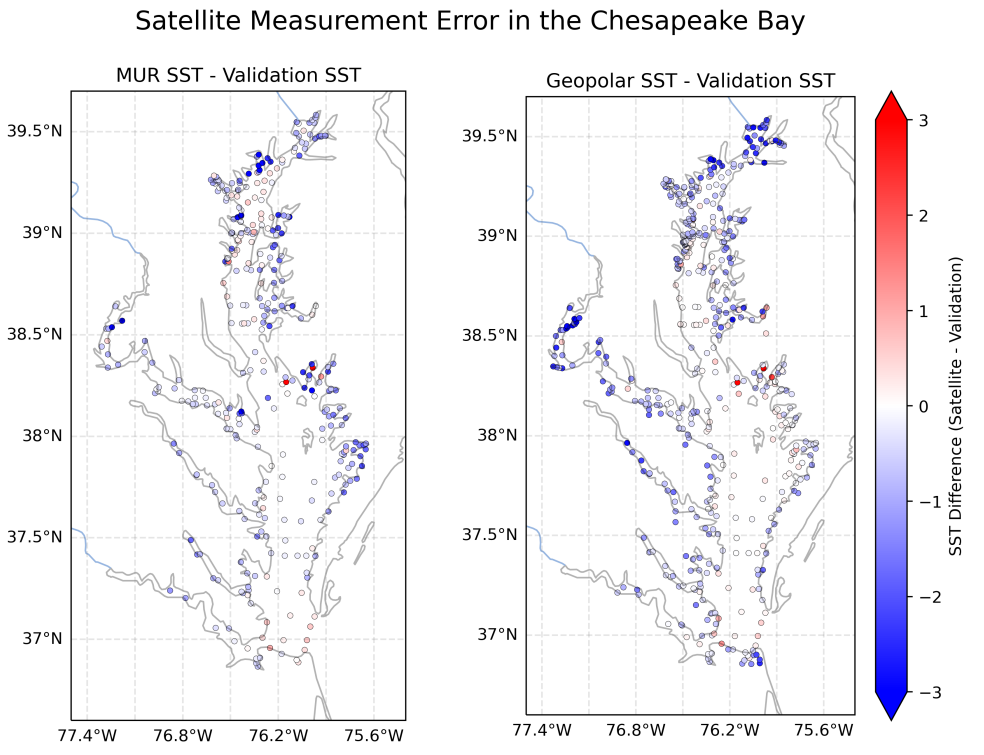

Figure 5. *Map of satellite SST errors for MUR and Geopolar datasets. The left panel shows MUR and the right panel shows Geopolar. The colorbar shows in situ minus satellite SST, such that negative (blue) values represent satellite SST underestimates of in situ temperature.*

3.1.3. Temporal Variability of Satellite Error

Another important form of bias in satellite errors is annual and seasonal variation. Hovmöller plots show that both satellite datasets have a seasonal trend in their errors (Figure 6). The satellites underestimate SST in the late spring and early summer and they overestimate SST in the late fall and early winter. Another notable pattern is that there is a long term trend present in the late summer of both datasets (MUR Jun-Sept and Geopolar Jul-Sept). The trend is stronger in MUR than in Geopolar. The impact of this trend is discussed in 3.1.4.

The strongest biases of either satellite dataset occur in early spring/summer MUR, about 2003-2005, underestimating SST as much as 4.5 degrees. Comparatively, Geopolar did not have any month with mean error larger than 3.5 degrees. Past analysis has noted this bias early in the MUR dataset and suggested that the effect is strongest in the upper bay (NOAA Coastwatch 2023).

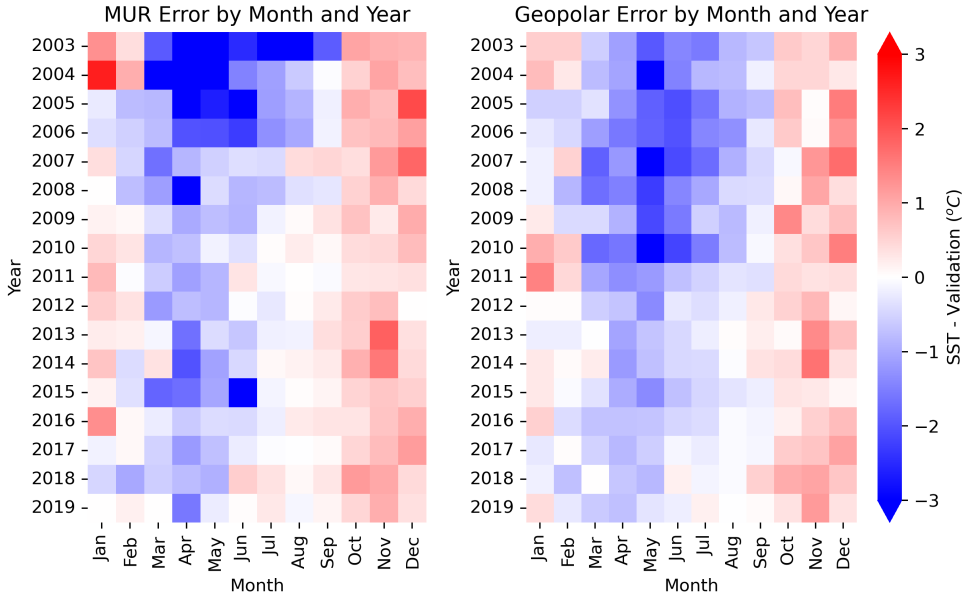

Figure 6. *The SST error for Geopolar and MUR by month and year.The left panel shows MUR SST and the right panel shows Geopolar SST. Each pixel corresponds to the average satellite error for all pixels in the bay during that year (x axis) and month (y axis). The colorbar shows satellite SST minus in situ measurements, such that negative (blue) values represent satellite SST underestimates of in situ temperature.*

3.1.4. Effects of Known SST Error on MHW Analysis

The SST signal is composed of a long term warming signal, a seasonal signal, and a higher frequency event (ex. MHW) signal:

$$T(t) = T_{long\ term} + T_{seasonal} + T_{high\ frequency\ events}$$

The calculation of MHWs is computed using temperature anomalies, meaning that the climatological signal is removed. As a result, while satellite SST datasets showed strong seasonal biases, this form of bias should not influence our results because the it is removed in the MHW calculation. Spatially each pixel is treated as an independent time series. Similarly, if spatial bias were consistent through time, the spatial patterns in temperature anomaly would be removed in the MHW calculation.

Conversely, any long term trend temporal in satellite error could have a significant impact on our results. It is primarily due to the impact of long term trend in satellite error that MHW analysis was performed using Geopolar SST instead of MUR. The early cold bias in MUR summer months could generate a false or overestimated long term warming signal that would impact results. Additionally, Geopolar has a slightly lower RMSE. Finally, past work has noted that when using climatologies shorter than 30 years, as this work is, impacts on MHW intensity and duration are larger if there is also a long term warming trend present (Schlegel, Oliver, Hobday, et al. 2019).

In summary, there are significant biases in the satellite SST. RMSE of both datasets was between 1.5 and 2^{o}C for SST. There are spatial and seasonal trends in the satellite datasets, but the removal of the baseline climatology in the MHW calculation means these types of satellite error will not impact MHW results. A long term temporal trend, on the other hand, could impact MHW results. The less prominent long term bias in the Geopolar dataset is the primary reason for using Geopolar SST for the MHW calculation.

3.2. Marine Heatwaves

3.2.1. Temporal MHW Characteristics

Globally, the frequency of MHW is increasing over time (Oliver, Donat, et al. 2018), an overall trend that is also apparent in the Chesapeake. Figure 7 shows the number of annual MHW events over time in the upper, middle, and lower sections of the Bay. All SST pixels over each of the three sections were averaged together to generate a single annual result. Large MHW dominate the time series, with major spikes in 2012, 2018, and 2020. These spikes are consistent with known large MHW in the Northwest Atlantic.

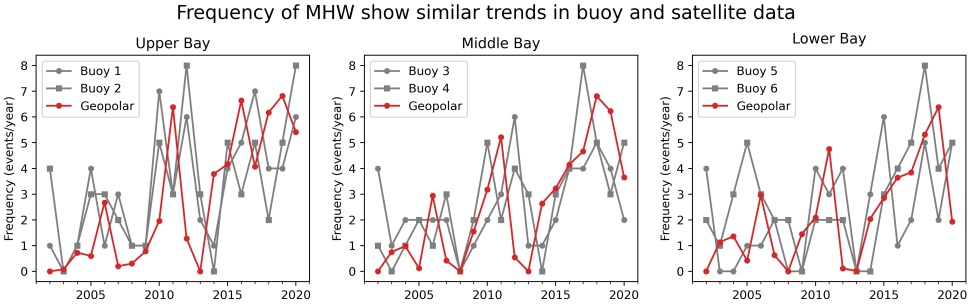

Figure 7. *Comparison of MHW frequency derived from satellite data with MHW frequency from buoys. Buoy derived MHW frequency was reported in Mazzini and Pianca 2022.*

The results from our analysis are shown alongside results from Mazzini and Pianca 2022, which derive MHW frequency from buoy data. There is good agreement between the buoy-derived MHW frequency and the satellite-derived MHW frequency. Mazzini and Pianca 2022 found that there were on average 2 MHW per year with an average duration of 11 days per year, resulting in an average of 22 MHW days per year. The satellite derived MHW produce consistent results, with a bay-wide average of 2.3 events per year and 10.8 days / event for a total of 25 MHW per year.

This comparison provides a further form of validation on our approach. It has enabled the reproduction of prior buoy-based work without using any buoys. The additional benefit of the satellite approach, however, is the ability to further existing understanding by looking at MHW spatial patterns.

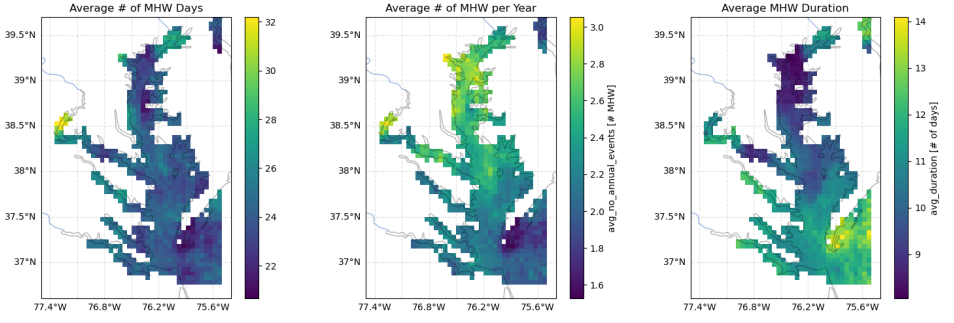

Figure 8. *The spatial distribution of the average number of MHW days per year using Geopolar SST. The average number of MHW days is calculated by multiplying the average number per year by the average duration.*

The bay-wide average of about 25 MHW days per year is overall spatially uniform. Considering only MHW days, however, obscures significant spatial variability in the duration and frequency of MHWs in

the bay. While there isn't spatial variability in the number of MHW days there is spatial variability in why there are MHW. Average number of annual MHW and MHW duration show a north-south gradient, ranging from about 2-3 MHW per year and MHW durations between 8 and 13 days. The average number of annual MHW is highest in the northern areas of the Bay while the average MHW duration is highest is the southernmost regions of the Bay. The north-south opposing gradient of these two fields leads to the uniform MHW days. To summarize, in the Chesapeake Bay there are longer, less frequent heatwaves in the southern regions of the Bay and shorter, more frequent MHW in the northern regions, leading to a uniform distribution of MHW days.

3.2.2. Marine Heatwave Characterization

The uniqueness of the satellite dataset is that it allows us to look at how MHW occurrences and characteristics change spatially. This spatial picture gives us a finer grained look at the development of MHW and could perhaps suggest physical mechanisms behind MHW development or decay. It could also give higher resolution insights into resource management.

The direct output of this analysis is 6 maps of MHW characteristics for the Chesapeake Bay (Figure 9). The 6 characteristics are:

- Average number of annual events
- Average MHW duration
- Average maximum intensity
- Average cumulative intensity
- Average rate of onset
- Average rate of decline

The dominant pattern in spatial variation in 4 of the 6 maps is a north-south gradient. The largest amount of spatial variation is present in MHW duration and number of annual events. Both of these characteristics increase by approximately 1.5-2 times between the lower and upper Bay. The highest values for average number of annual events are in the northern Bay and decrease southward. The inverse is true for average MHW duration. The exception to this north-south trend is areas of high river influence, including the upper bay where the Susquehanna River enters the Bay. It is not clear if this represents a true finding in the data or if the is a reflection of high satellite error rates in the river outflow regions. The average maximum intensity signal is also similar to areas of river outflow and may likewise may be related to satellite error structure (see Section 3.1.2).

Other MHW characteristics showed spatial variation with a less consistent but equally informative pattern. Rate of onset showed an approximately 1.5 times difference between the highest and lowest values in the Bay, with some longitudinal gradient. Relative to rate of onset rate of decline is more uniform in the main stem of the bay. This may suggest different mechanisms controlling the develop and the decay of MHW. Further investigation into the finer scale spatial structure of the rates of onset and decline could be an avenue of further research.

Another noteworthy spatial trend is seen in cumulative intensity. Cumulative intensity is a reflection of two aspects of a heatwave: duration and intensity. A MHW can have high cumulative intensity either because the MHW lasts for a long time, it is very hot, or both. In the Chesapeake Bay, MHW cumulative intensity is more strongly influenced by duration than by maximum intensity (Figure 9). This relationship is likely a reflection of the larger spatial variation in average MHW duration than in average maximum intensity. The range of duration is about 50% of the minimum value, whereas the intensity range is only about 20%.

Contributions to cumulative intensity are of importance for resource management. In general sustained stress is more detrimental to organisms than quick temperature increases. We hope knowledge of the role of duration in cumulative intensity will be of use to local policy makers.

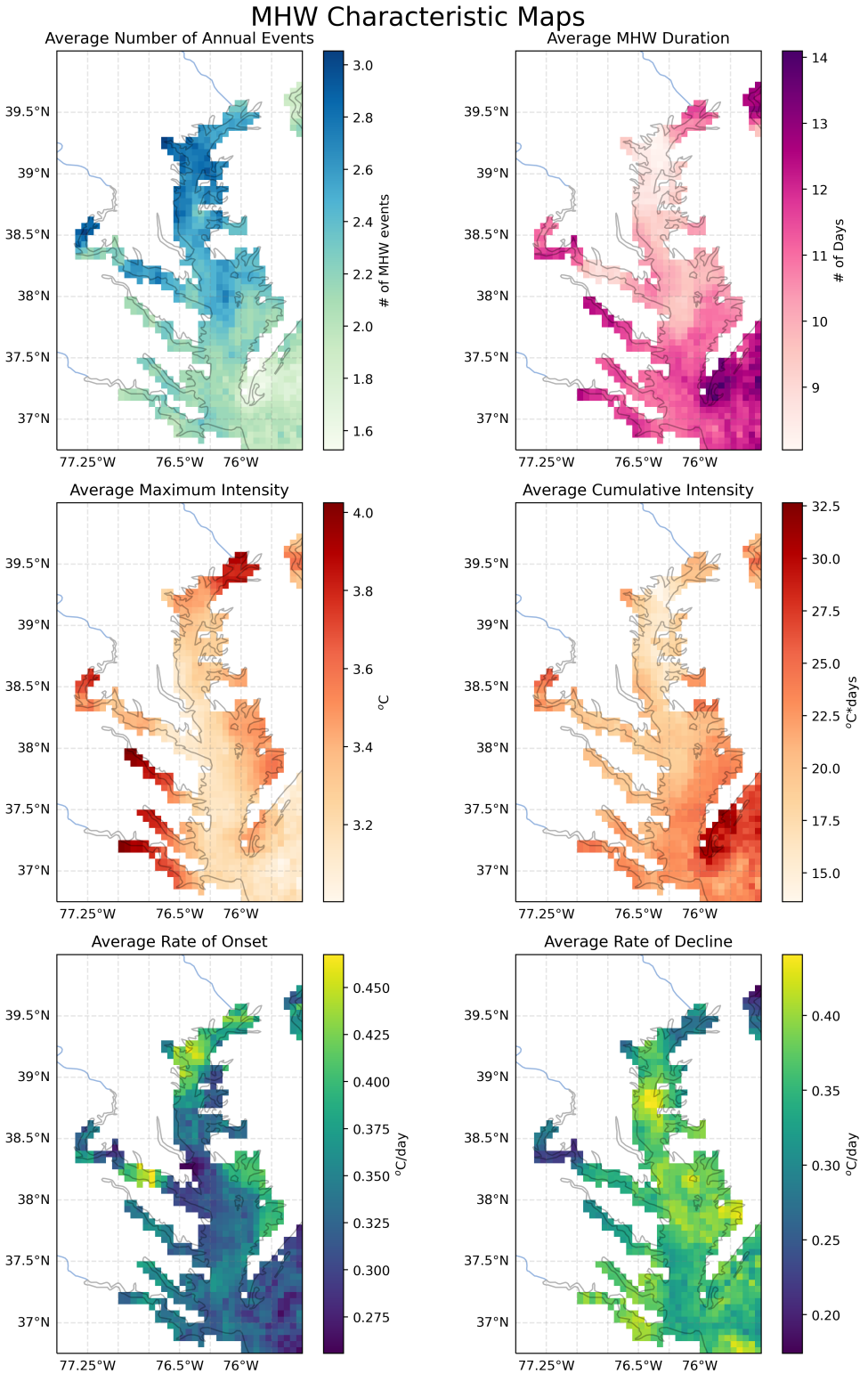

Figure 9. *Spatial maps showing the distribution of 6 MHW characteristics. Maps show an aggregation (either sum or average) of across time for each pixel. The aggregation process is detailed in Figure 3.*

3.2.3. Spatial Variability in Long Term MHW Trends

To aid in understanding temporal trends in the Bay an analysis of long term changes in MHW characteristics is performed. To calculate the long term trend each pixel is treated as an independent time series. Each time series is grouped into annual bins with the number of MHW in that year and the average duration of all the MHW in that year. These annual points were then fit to a linear trend and the slope and p value were calculated for the 20 year times series. Figure 10 shows the slope from this regression for each pixel. Only pixels whose p-value is less than 0.05 are shown.

Almost the entire Bay is experiencing significant increases in the number of annual MHW events (Figure 10). The largest values are about 0.5 event / year, which is equivalent to about 5 additional MHW events per decade. Average MHW duration, on the other hand, only shows a significant long term trend in the upper and middle bay and in the river regions. The largest changes in MHW duration occur in the upper bay and are equivalent to MHW which are about 6-7 days longer per decade. MHW duration increases in the middle Bay are about 4-5 days per decade. This is a substantial increase given that the average MHW duration is lowest in those regions (about 9 days), suggesting a doubling of MHW duration in this sector of the bay over the course of 2 decades.

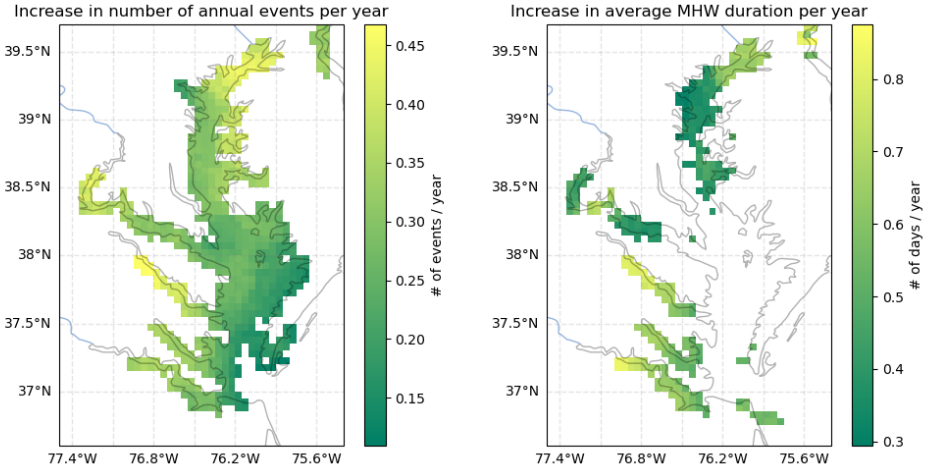

Figure 10. *Long term trends in MHW characteristics. Plots show the slope of a linear regression on each pixel. Only those pixels whose linear regression had a p value of < 0.05 were included. Left plot shows the average annual increase in MHW frequency and the right plot shows the increase in average duration per year.*

4. Conclusion

In this study satellite data was used to investigate MHWs in the Chesapeake Bay. Two SST sources, NASA MUR and NOAA Geopolar, were compared against in situ measurements. Both satellite datasets were found to have similar forms of error, but the lower RMSE and less prominent long term trend motivated the use of Geopolar for the MHW calculation. Validation work such as this is critical for accurate interpretation of global SST datasets in coastal zones. Using satellite SST in the narrow Chesapeake pushes the limits of these satellite datasets. This validation was possible because of the availability of in situ validation data, but this resource is not available in all other estuaries. Successful use of satellite SST in the Chesapeake supports the possibility that satellite SST may also be a useful tool for studying temperature in other large estuaries where independent validation experiments may not be possible due to a lack of in situ data.

MHW characteristic maps reveal significant spatial variation, where the dominant trend is a north to south gradient. Spatial structure reveals that cumulative intensity is dominated by MHW duration, not max intensity. This result, coupled with the strong bay wide variation in MHW duration, highlight MHW duration as a key MHW characteristic in the Chesapeake Bay. These insights can only be derived by considering the spatial structure of MHW and highlight the importance of satellite-based MHW analysis. Temporal MHW show increases in MHW over time and an average of 25 MHW days per year bay-wide. Increases in MHW days in the lower bay can be as high as almost 5 additional annual events per decade, a near doubling over the 20 year period. This highlights the significance of extreme events long term change. Satellite-derived MHW analysis is consistent with past buoy-wide analysis, giving confidence in the accuracy of this new technique.

Future work could focus on investigation of satellite errors in the river inflow regions. Here a qualitative analysis of the relative contribution of satellite error biases provided confidence in the MHW technique, but a quantitative analysis could provide a more in depth understanding. If the spatial signal observed in the satellite data is in fact a true MHW signal this could have significant impacts for resource management. Additionally, future analysis could focus spatial patterns related to MHW mechanisms of development and decline. Past work in the North Atlantic suggested atmospheric mechanisms to be the most influential mechanism in MHW development while ocean processes to be the more influential mechanism in MHW decline (Schlegel, Oliver, and Chen 2021). Rate of onset and decline in the Chesapeake Bay showed the finest scale spatial structure, and differences in their distributions could be related to mechanistic influence.

The Chesapeake Bay is the largest estuary in the US and the impacts of a warming climate have societal and economic impact. This work provides validation of satellite SST in the Bay allowing future researchers to more accurately understand results derived using SST in the Bay. Spatial variation in MHW characteristics highlights the importance of spatial structure in the Bay and could provide insight into physical MHW mechanisms.

Acknowledgments. This work builds off the research of Skylar Lama (University of Maryland, 2021-2022). We are grateful to have been able to continue her initial investigation into Chesapeake Bay marine heatwaves.

References

Beggs, Helen (Mar. 2020). *Chapter 14: Temperature, In: Earth Observation: Data, Processing and Applications. Volume 3B: Applications – Surface Waters (Eds. Harrison, B.A., Anstee, J.A., Dekker, A., Phinn, S., Mueller, N., Byrne, G.) CRCSI, Melbourne.*

Bilkovic, Donna Marie et al. (Jan. 1, 2019). "Chapter 15 - Chesapeake Bay". In: *World Seas: an Environmental Evaluation (Second Edition)*. Ed. by Charles Sheppard. Academic Press, pp. 379–404. ISBN: 978-0-12-805068-2. DOI: 10.1016/B978-0-12-805068-2.00019-X. URL: https://www.sciencedirect.com/science/article/pii/B978012805068200019X (visited on 05/21/2023).

Bulgarelli, Barbara and Giuseppe Zibordi (May 1, 2018). "On the detectability of adjacency effects in ocean color remote sensing of mid-latitude coastal environments by SeaWiFS, MODIS-A, MERIS, OLCI, OLI and MSI". In: *Remote Sensing of Environment* 209, pp. 423–438. ISSN: 0034-4257. DOI: 10.1016/j.rse.2017.12.021. URL: https://www.sciencedirect.com/science/article/pii/S0034425717305965 (visited on 05/26/2023).

Chin, Toshio Michael, Jorge Vazquez-Cuervo, and Edward M. Armstrong (Oct. 1, 2017). "A multi-scale high-resolution analysis of global sea surface temperature". In: *Remote Sensing of Environment* 200, pp. 154–169. ISSN: 0034-4257. DOI: 10.1016/j.rse.2017.07.029. URL: https://www.sciencedirect.com/science/article/pii/S0034425717303462 (visited on 05/21/2023).

Du, Jiabi et al. (July 2018). "Worsened physical condition due to climate change contributes to the increasing hypoxia in Chesapeake Bay". In: *Science of The Total Environment* 630, pp. 707–717. ISSN: 00489697. DOI: 10.1016/j.scitotenv.2018.02.265. URL: https://linkinghub.elsevier.com/retrieve/pii/S004896971830665X (visited on 02/15/2023).

Duan, Si-Bo et al. (Aug. 1, 2020). "Influence of adjacency effect on high-spatial-resolution thermal infrared imagery: Implication for radiative transfer simulation and land surface temperature retrieval". In: *Remote Sensing of Environment* 245, p. 111852. ISSN: 0034-4257. DOI: 10.1016/j.rse.2020.111852. URL: https://www.sciencedirect.com/science/article/pii/S0034425720302224 (visited on 05/26/2023).

Hinson, Kyle E. et al. (Dec. 2022). "Extent and Causes of Chesapeake Bay Warming". In: *J American Water Resour Assoc* 58.6, pp. 805–825. ISSN: 1093-474X, 1752-1688. DOI: 10.1111/1752-1688.12916. URL: https://onlinelibrary.wiley.com/doi/10.1111/1752-1688.12916 (visited on 02/15/2023).

Hobday, Alistair J. et al. (Feb. 1, 2016). "A hierarchical approach to defining marine heatwaves". In: *Progress in Oceanography* 141, pp. 227–238. ISSN: 0079-6611. DOI: 10.1016/j.pocean.2015.12.014. URL: https://www.sciencedirect.com/science/article/pii/S0079661116000057 (visited on 01/23/2023).

Lefcheck, Jonathan S. et al. (2017). "Multiple stressors threaten the imperiled coastal foundation species eelgrass (Zostera marina) in Chesapeake Bay, USA". In: *Global Change Biology* 23.9. _eprint: https://onlinelibrary.wiley.com/doi/pdf/10.1111/gcb.13623, pp. 3474–3483. ISSN: 1365-2486. DOI: 10.1111/gcb.13623. URL: https://onlinelibrary.wiley.com/doi/abs/10.1111/gcb.13623 (visited on 05/21/2023).

Maturi, Eileen et al. (May 1, 2017). "A New High-Resolution Sea Surface Temperature Blended Analysis". In: *Bulletin of the American Meteorological Society* 98.5. Publisher: American Meteorological Society Section: Bulletin of the American Meteorological Society, pp. 1015–1026. ISSN: 0003-0007, 1520-0477. DOI: 10.1175/BAMS-D-15-00002.1. URL: https://journals.ametsoc.org/view/journals/bams/98/5/bams-d-15-00002.1.xml (visited on 05/21/2023).

Mazzini, Piero L. F. and Cassia Pianca (2022). "Marine Heatwaves in the Chesapeake Bay". In: *Frontiers in Marine Science* 8. ISSN: 2296-7745. URL: https://www.frontiersin.org/articles/10.3389/fmars.2021.750265 (visited on 01/23/2023).

NOAA Coastwatch (2023). personal communication. URL: https://eastcoast.coastwatch.noaa.gov/cw_podaac-mur_valid.php (visited on 05/22/2023).

Oliver, Eric C. J., Michael T. Burrows, et al. (2019). "Projected Marine Heatwaves in the 21st Century and the Potential for Ecological Impact". In: *Frontiers in Marine Science* 6. ISSN: 2296-7745. URL: https://www.frontiersin.org/articles/10.3389/fmars.2019.00734 (visited on 01/23/2023).

Oliver, Eric C. J., Markus G. Donat, et al. (Apr. 10, 2018). "Longer and more frequent marine heatwaves over the past century". In: *Nature Communications* 9.1, p. 1324. ISSN: 2041-1723. DOI: 10.1038/s41467-018-03732-9. URL: https://doi.org/10.1038/s41467-018-03732-9.

Rahmstorf, Stefan and Dim Coumou (Nov. 2011). "Increase of extreme events in a warming world". In: *Proc. Natl. Acad. Sci. U.S.A.* 108.44, pp. 17905–17909. ISSN: 0027-8424, 1091-6490. DOI: 10.1073/pnas.1101766108. URL: https://pnas.org/doi/full/10.1073/pnas.1101766108 (visited on 02/15/2023).

Schlegel, Robert W., Eric C. J. Oliver, and Ke Chen (2021). "Drivers of Marine Heatwaves in the Northwest Atlantic: The Role of Air–Sea Interaction During Onset and Decline". In: *Frontiers in Marine Science* 8. ISSN: 2296-7745. URL: https://www.frontiersin.org/articles/10.3389/fmars.2021.627970 (visited on 05/26/2023).

Schlegel, Robert W., Eric C. J. Oliver, Alistair J. Hobday, et al. (Nov. 28, 2019). "Detecting Marine Heatwaves With Sub-Optimal Data". In: *Front. Mar. Sci.* 6, p. 737. ISSN: 2296-7745. DOI: 10.3389/fmars.2019.00737. URL: https://www.frontiersin.org/article/10.3389/fmars.2019.00737/full (visited on 03/06/2023).

Smith, Kathryn E., Michael T. Burrows, Alistair J. Hobday, Nathan G. King, et al. (2023). "Biological Impacts of Marine Heatwaves". In: *Annual Review of Marine Science* 15.1. _eprint: https://doi.org/10.1146/annurev-marine-032122-121437, pp. 119–145. DOI: 10.1146/annurev-marine-032122-121437. URL: https://doi.org/10.1146/annurev-marine-032122-121437 (visited on 01/23/2023).

Smith, Kathryn E., Michael T. Burrows, Alistair J. Hobday, Alex Sen Gupta, et al. (Oct. 22, 2021). “Socioeconomic impacts of marine heatwaves: Global issues and opportunities”. In: *Science* 374.6566, eabj3593. ISSN: 0036-8075, 1095-9203. DOI: 10.1126/science.abj3593. URL: https://www.science.org/doi/10.1126/science.abj3593 (visited on 02/15/2023).